# Expanded View Figures

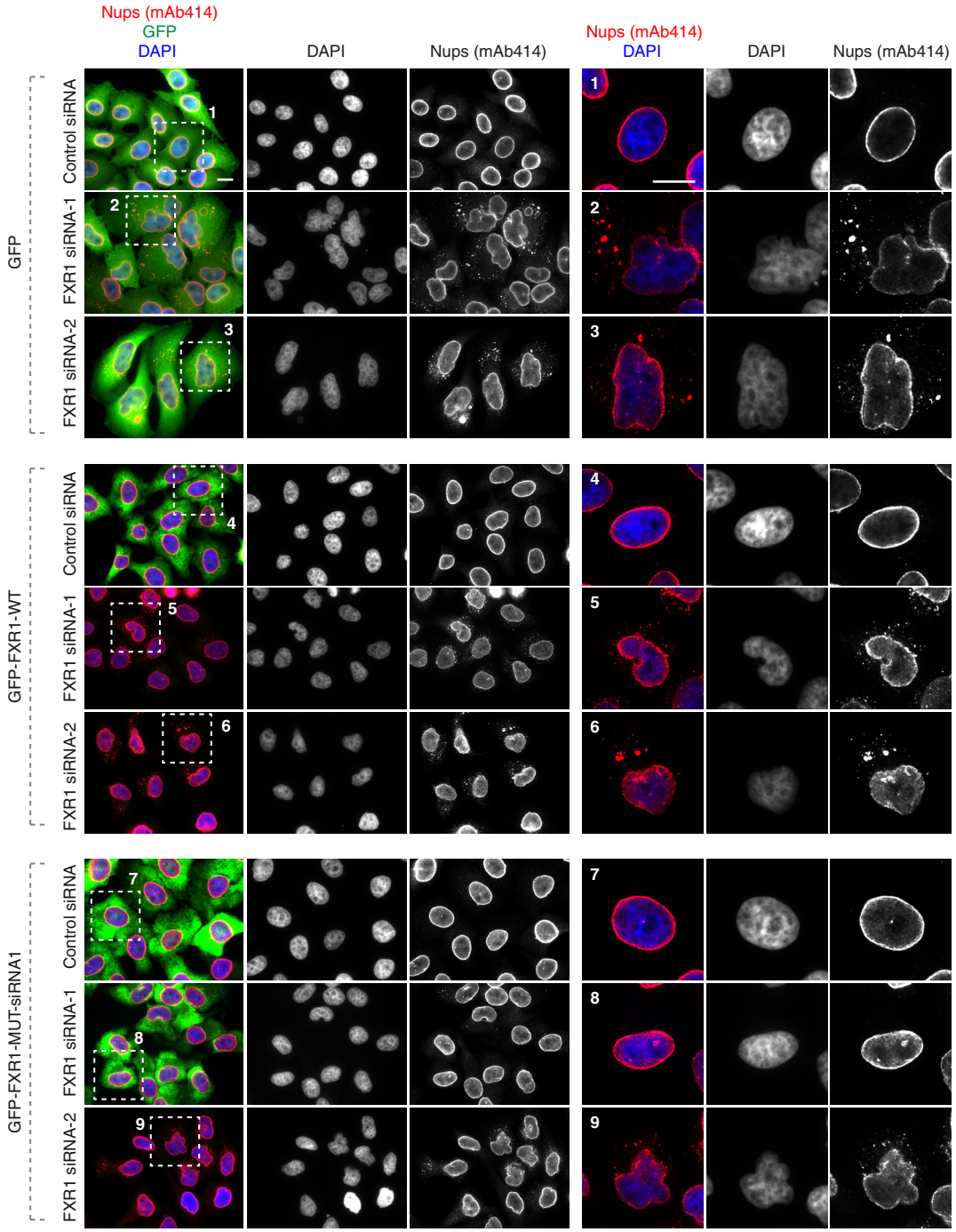


**Figure EV1. FXR1 specifically controls cytoplasmic Nups and nuclear shape.**

HeLa cells stably expressing GFP, GFP-FXR1 wild type (WT) and GFP-FXR1 mutated in the sequence recognized by FXR1 siRNA-1 (GFP-FXR1-MUT-siRNA1) were treated with the indicated siRNAs, synchronized by double thymidine block and released for 24 h and analysed by immunofluorescence microscopy for mAb414 (related to Figs 2B and 3B and C). Scale bars are 5 μm.

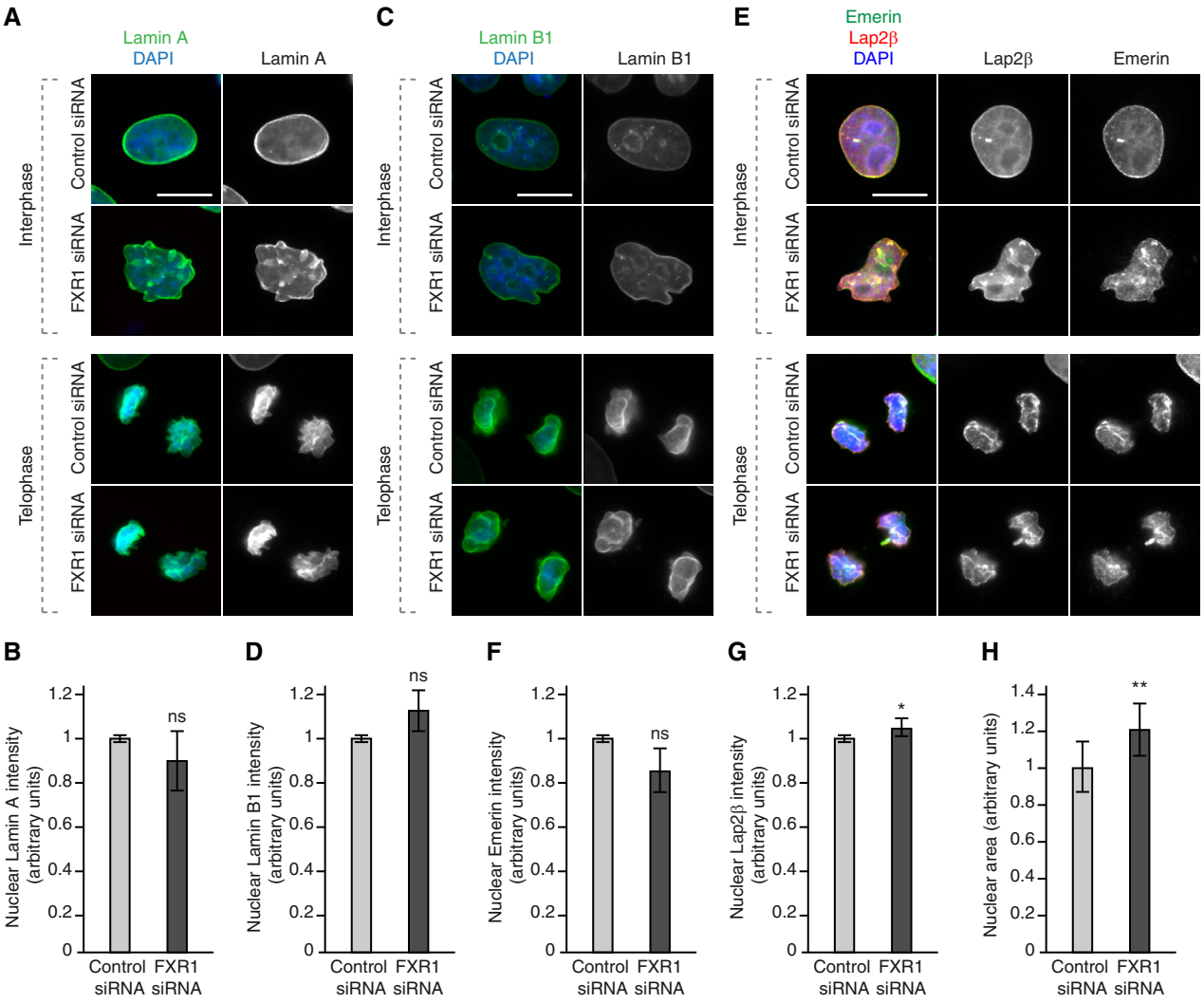


**Figure EV2. FXR1 does not drive recruitment of lamina-associated proteins.**

A–H HeLa cells were treated with the indicated siRNAs, synchronized by double thymidine block and released for 9 (telophase) and 12 (interphase) h and analysed by immunofluorescence microscopy. The nuclear intensity of Lamin A (B), Lamin B1 (D), Emerin (F) and Lap2β (G) was quantified, and 2,000 cells were analysed (mean ± SD, $*P < 0.05$; ns, non-significant; $N = 3$). The nuclear area was quantified (H), and 3,300 cells were analysed (mean ± SD, $**P < 0.01$; $N = 5$).

Data information: Scale bars are 5 μm. Statistical significance was assessed by one-sample two-tailed Student's *t*-test.

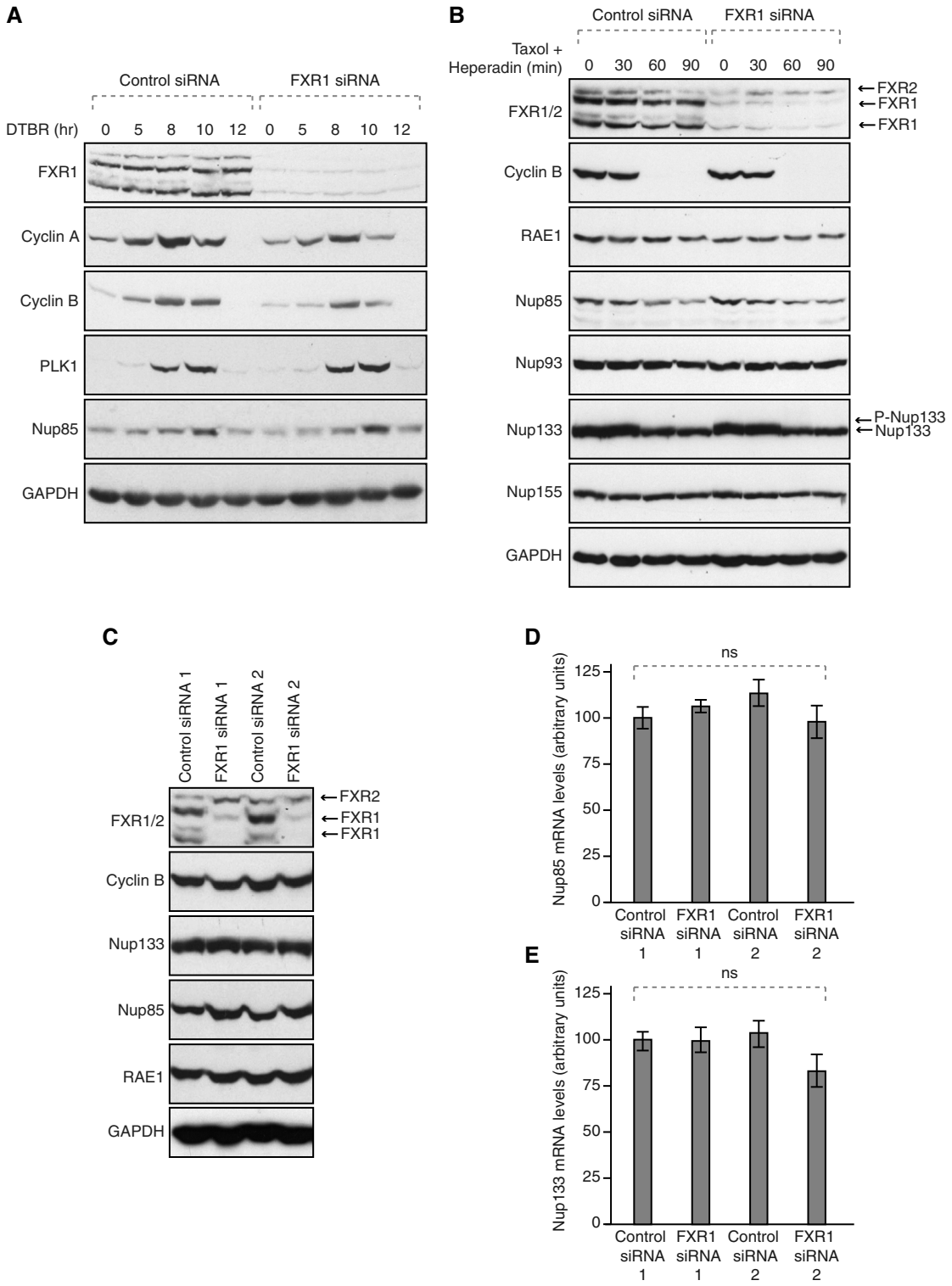


**Figure EV3.**

**Figure EV3. FXR1 does not regulate mitotic exit and protein levels of several Nups.**

A HeLa cells were treated with the indicated siRNAs, synchronized by double thymidine block and released for the indicated times (hours) and analysed by Western blot.

B HeLa cells were treated with the indicated siRNAs, synchronized by Hesperadin release from mitotic arrest induced by Taxol and analysed by Western blot. Arrows point to FXR1 isoforms, FXR2 and phosphorylated (P-Nup133) and unmodified form of Nup133, respectively.

C HeLa cells were treated with the indicated siRNAs, synchronized by double thymidine block, released in interphase and analysed by Western blot. Arrows point to FXR1 isoforms and FXR2 protein.

D, E HeLa cells were treated with the indicated siRNAs, and mRNA levels of Nup85 (D) and Nup133 (E) were analysed by quantitative real-time PCR (mean ± SD, ns, non-significant; $N = 3$).

Data information: Statistical significance was assessed by two-tailed Student's *t*-test.

Source data are available online for this figure.




© 2020 The Authors

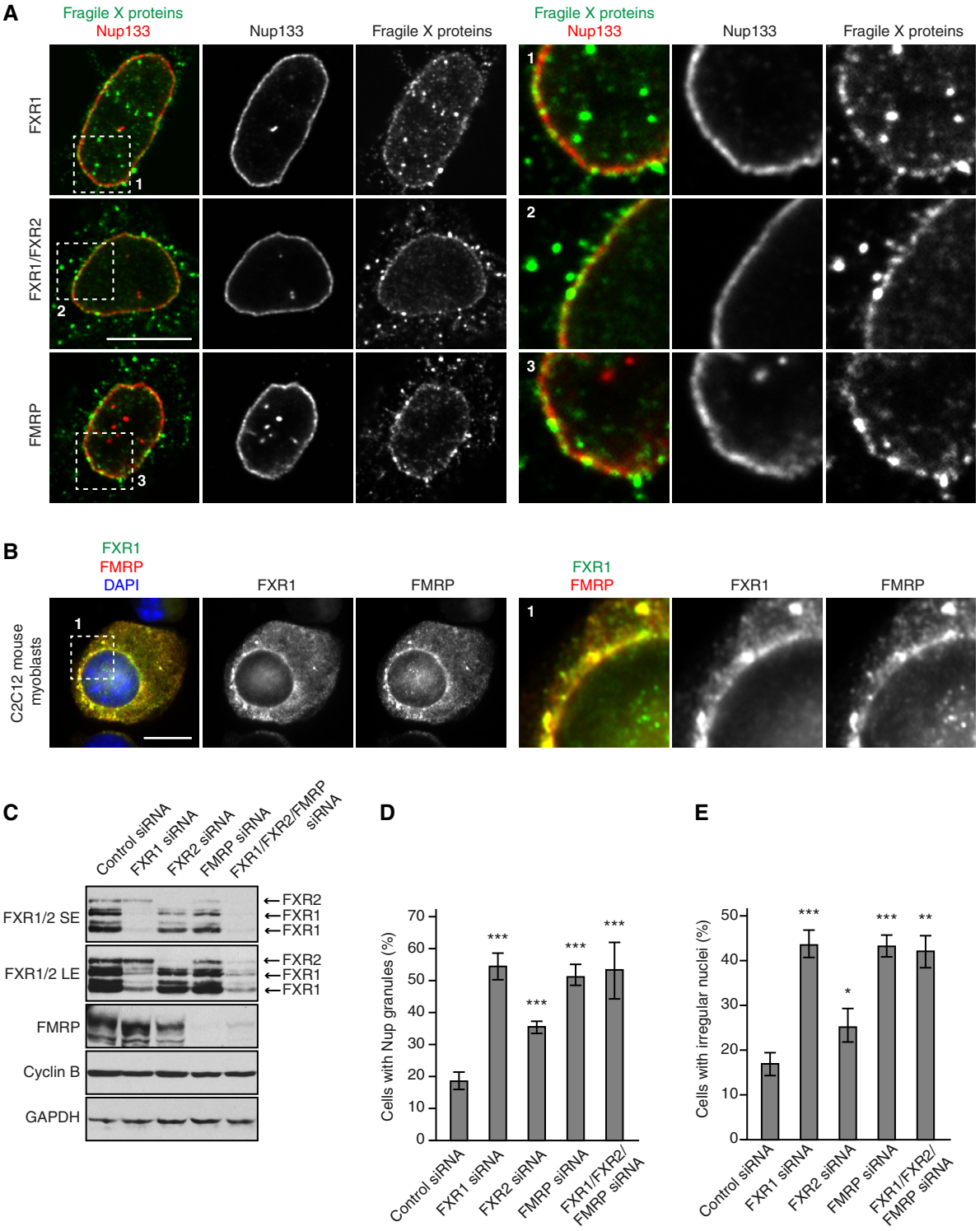


**Figure EV4.**

**Figure EV4. FXR protein family members localize to NE and regulate cytoplasmic Nups.**

A, B HeLa cells (A) and mouse C2C12 myoblasts (B) were analysed by immunofluorescence microscopy for FXR1, FXR1 + 2 and FMRP. The magnified framed regions are shown in the corresponding numbered panels.

C–E HeLa cells were treated with the indicated siRNAs, synchronized by double thymidine block and released for 12 h and analysed by Western blot (SE—short exposure, LE—long exposure) (C) and immunofluorescence microscopy (D, E). The percentage of cells with cytoplasmic nucleoporin granules (D) and irregular nuclei (E) was quantified, and 900 cells were analysed (mean ± SD, $*P < 0.05$; $**P < 0.01$; $***P < 0.001$; $N = 3$).

Data information: Scale bars are 5 μm. Statistical significance was assessed by one-way ANOVA test with Dunnett's correction (D, E).
Source data are available online for this figure.

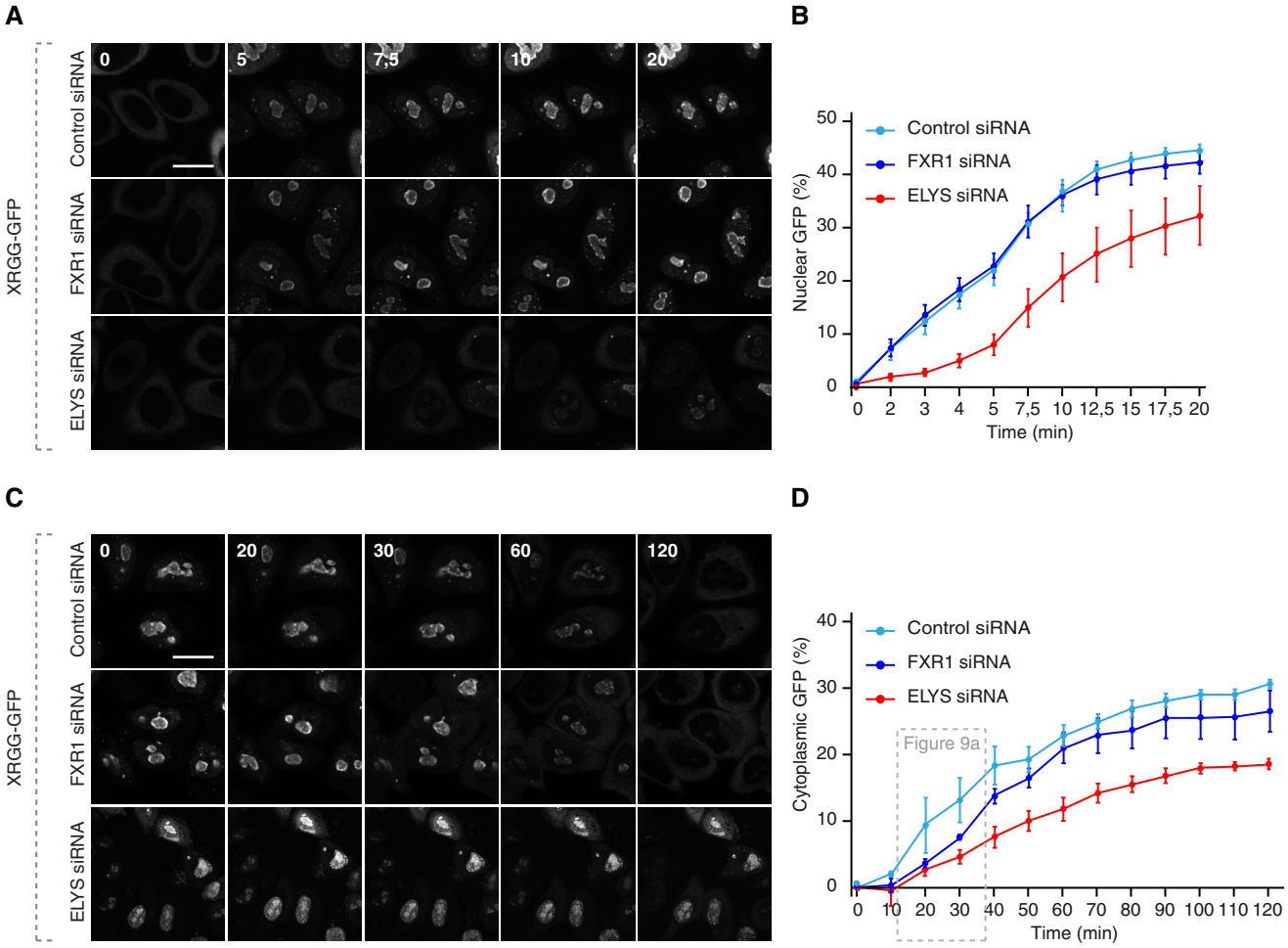


**Figure EV5. FXR1 protein does not regulate steady-state nucleocytoplasmic transport.**

A, B HeLa cells were transfected with the import reporter plasmid XRGG-GFP, treated with the indicated siRNAs and synchronized in early G1 phase by Monastrol release. Dexamethasone-induced nuclear import of XRGG-GFP was analysed by live video spinning disc confocal microscopy (A). The selected frames of the movies are depicted, and time is shown in min. The increase in the percentage of nuclear XRGG-GFP over time was quantified in (B), and 247 cells were analysed (mean ± SEM, $N = 3$).

C, D HeLa cells were treated as in (A, B), and dexamethasone was added for 3 h to induce XRGG-GFP nuclear import. Following washout, the nuclear export of XRGG-GFP was analysed by live video spinning disc confocal microscopy (C). The selected frames of the movies are depicted, and time is shown in min. The increase in the percentage of cytoplasmic XRGG-GFP over time was quantified in (D), and 199 cells were analysed (mean ± SEM; $N = 3$). The distribution of cells with cytoplasmic XRGG-GFP at the time points corresponding to early G1 cell cycle stage (20 and 30 min) are depicted in Fig 9A.

Data information: Scale bars are 5 μm.